의학석사 학위논문

동물 모델에서 5-아미노레불린산 유도 헴 합성을 이용한 U-87 인간 교모세포종의 T2* 자기공명영상

T2* Magnetic resonance imaging of U-87 human glioblastoma using 5-aminolevulinic acid induced heme synthesis in an animal model

2013년 2월

서울대학교 대학원

의학과 영상의학 석사과정

김동현

A thesis of the Master's degree

T2* Magnetic resonance imaging of U-87 human glioblastoma using 5-aminolevulinic acid induced heme synthesis in an animal model

동물 모델에서 5-아미노레불린산 유도 헴 합성을 이용한 U-87 인간 교모세포종의 T2* 자기공명영상

February 2013

The Department of Radiology,

Seoul National University

College of Medicine

Dong Hyun Kim

동물 모델에서 5-아미노레불린산 유도 헴 합성을 이용한 U-87 인간 교모세포종의 $T2^*$ 자기공명영상

지도교수 한 문 희

이 논문을 의학석사 학위논문으로 제출함

2012 년 10 월

서울대학교 대학원

의학과 영상의학 전공

김 동 현

김동현의 의학석사 학위논문을 인준함

2012 년 12 월

위 원 장 (인)

부위원장 (인)

위 원 (인)

T2* Magnetic resonance imaging of U-87 human glioblastoma using 5-aminolevulinic acid induced heme synthesis in an animal model

by

Dong Hyun Kim

A thesis submitted to the Department of Radiology in partial fulfillment of the requirements for the Degree of Master of Science in Radiology at Seoul National University College of Medicine

December 2012

Approved by Thesis Committee:

Professor _____ **Chairman**

Professor _____ **Vice chairman**

Professor _____

학위논문 원문제공 서비스에 대한 동의서

본인의 학위논문에 대하여 서울대학교가 아래와 같이 학위논문 제공하는 것에 동의합니다.

1. 동의사항

① 본인의 논문을 보존이나 인터넷 등을 통한 온라인 서비스 목적으로 복제할 경우 저작물의 내용을 변경하지 않는 범위 내에서의 복제를 허용합니다.

② 본인의 논문을 디지털화하여 인터넷 등 정보통신망을 통한 논문의 일부 또는 전부의 복제.배포 및 전송 시 무료로 제공하는 것에 동의합니다.

2. 개인(저작자)의 의무

본 논문의 저작권을 타인에게 양도하거나 또는 출판을 허락하는 등 동의 내용을 변경하고자 할 때는 소속대학(원)에 공개의 유보 또는 해지를 즉시 통보하겠습니다.

3. 서울대학교의 의무

① 서울대학교는 본 논문을 외부에 제공할 경우 저작권 보호장치(DRM)를 사용하여야 합니다.

② 서울대학교는 본 논문에 대한 공개의 유보나 해지 신청 시 즉시 처리해야 합니다.

논문 제목 : 동물 모델에서 5-아미노레불린산 유도 헴 합성을 이용한 U-87 인간 교모세포종의 T2* 자기공명영상

학위구분: **석사 ∨□ · 박사 □**

학 과: 의학과 영상의학 전공

학 번: 2011-21824

연 락 처:서울대학교병원 영상의학과

저 작 자: 김 동 현 (인)

제 출 일: 2013 년 2 월 4 일

서울대학교총장 귀하

Abstract

Background and Purpose: This study developed a new technology for visualizing malignant foci in brain tumors using magnetic resonance imaging (MRI). Administration of 5-aminolevulinic acid (5-ALA) causes an accumulation of fluorescent protoporphyrin IX (PpIX) in malignant gliomas, which can be used as a marker for the detection of malignant foci in diffusely infiltrating gliomas. Here, we demonstrate that heme synthesis induced by 5-ALA could be detected using in vivo MRI. In this approach, the heme is made superparamagnetic as mitochondrial ferrochelatase (FECH) incorporates ferrous iron into PpIX, and cells that accumulate PpIX act as the MRI contrasting agent by employing endogenous iron, thereby simplifying the identification of malignant foci.

Materials and Methods: In vitro experiment, we measured intracellular iron, heme, PpIX and FECH at 1, 24 and, 48 h after in the human glioblastoma cell line U-87 treated with or without 5-ALA.

In vivo experiment, a total of 10 mice with orthotopic brain tumors were used in this study. The mice received an oral administration of 5-ALA (n = 6; 5-ALA group) or normal saline (n = 4; control group) 24 h before MRI. MRI was administered before and 24 h after the oral intake of 5-ALA or normal saline. For the analysis of T_2* in the brain tumors, we generated T_2* maps of the ROIs using pixel-by-pixel analyses in MATLAB™ (MathWorks Inc.). Then, mice were sacrificed for histology and measurement of intratumoral iron levels.

Results: In vitro experiment, the intracellular iron and heme levels of cells exposed to 5-ALA were higher than those of control cells at 24 h (1.95 ± 0.07 vs. 1.67 ± 0.07 μg/mg, $P < 0.05$ and 1.19 ± 0.07 vs. 0.86 ± 0.11

μg/mg, $P < 0.001$). The intracellular PpIX concentration was increased at 1 h after exposure to 5-ALA but had decreased by 24 and 48 h. Treatment with 5-ALA resulted in the greatest intracellular concentration of FECH at 24 h posttreatment (0.315 ng/mg protein, $P < 0.01$), and the intracellular concentration of FECH at 24, 48 h was higher in cells treated with 5-ALA as compared those untreated ($P < 0.001$).

In vivo experiment, the mean T_2* value of U-87 glioblastomas treated with 5-ALA was lower than that of control tumors, which received normal saline (14.9 ± 1.2 vs. 21.4 ± 2.6 ms, $P < 0.0001$). The mean T_2* value of brain tumors significantly decreased following treatment with 5-ALA (20.6 ± 1.1 vs. 14.9 ± 1.2 ms, $P < 0.0001$). Intratumoral iron levels also showed a significant difference in the mean concentration of iron between the control animals and the 5-ALA-treated animals (41.4 ± 0.9 μg/g vs. 60.1 ± 2.2 μg/g, $P < 0.0001$).

Conclusion: After administering an oral dose of 5-ALA, we report that 5-ALA dependent changes in T_2* were hypointense and could be detected in brain tumors by MRI. Thus, this technology is suitable for the in vivo identification of malignant foci in diffusely infiltrating gliomas and can be used for numerous biomedical applications in human studies.

……

Keywords: 5-aminolevulinic acid
glioblastoma
protoporphyrin IX
heme
magnetic resonance imaging

Student number: 2011-21824

Contents

List of Figures

Introduction

The intratumoral heterogeneity of gliomas poses a risk for the histological undergrading of these tumors, which leads to a delay in the administration of adjuvant treatment. Thus, intraoperative identification and sampling of the most malignant area are crucial (1). Although magnetic resonance imaging (MRI) is the most popular modality for the preoperative detection of anaplastic foci, signal anomalies limit the reliability of grading glial tumors, even with the aid of gadolinium contrasting agents (2, 3). Advanced MRI techniques such as diffusion-weighted imaging, perfusion-weighted imaging, and magnetic resonance spectroscopy enable the detection of anaplastic foci in gliomas (4–6), although the quantitative values obtained from these image sequences frequently overlap in their characterization of low- and high-grade gliomas.

Several studies have sought to overcome the limitations of anaplastic foci detection, including the use of isotopically labeled amino acid tracers to enhance imaging modalities such as ^{11}C-methionine-PET (MET-PET) or ^{18}F-fluoroethyl-L-tyrosine-PET (FET-PET) (7, 8). In the case of MET-PET, histological analysis confirmed that voxels with maximum tracer uptake (PETmax) represent the most malignant tumor areas (9–12). However, PET exposes the patient to radiation and is only available in highly specialized neurooncological centers.

Recently, 5-aminolevulinic acid (5-ALA) was identified as a new marker for the detection of malignant foci in diffusely infiltrating gliomas (1). 5-ALA is a nonfluorescent pro-drug that leads to the intracellular accumulation of fluorescent protoporphyrin IX (PpIX) in malignant

glioma cells (13). The fluorescent signal derived from PpIX provides enhanced contrast between tumors and normal tissue, enabling more complete resections and improving the progression-free survival rate in patients with malignant glioma (14). However, in low-grade gliomas, the utility of 5-ALA fluorescence has not been studied (15–17).

The polymerization of eight 5-ALA monomers results in the synthesis of PpIX, which is critical for heme synthesis (18, 19). In the final stages in heme synthesis, iron enters the heme cycle when mitochondrial ferrochelatase (FECH) incorporates ferrous iron (Fe^{2+}) into PpIX to generate heme (20). Synthesized heme is degraded by heme oxygenase to produce equimolar quantities of biliverdin, free Fe^{2+}, and carbon monoxide (21). Previous studies (22, 23) have shown that high iron concentrations as a result of heme accumulation appear dark (hypointense) on T_2-weighted images due to the susceptibility effect of iron. However, there was no previous study, using 5-ALA induced heme synthesis in glioma for the noninvasive detection of malignant portion with T_2-weighted MRI.

Here, we report the use of 5-ALA for the noninvasive detection of malignant glioma in vivo using MRI. We hypothesized that 5-ALA would selectively accumulate in malignant glioma cells and be converted to heme, which could then be detected by MRI. To this end, we developed an orthotropic mouse brain tumor model using the human glioblastoma cell line U-87MG. In addition, we confirmed the accumulation of iron in malignant glioma cells using laser ablation-inductively coupled plasma-mass spectrometry (LA-ICP-MS).

Materials and Methods

In Vitro Experiments.

Measurement of PpIX in cells without exposure to FAC.

For Fluorescence microscopy, U-87 (1×10^5) cells were incubated in six-well plates, which were wrapped in aluminum foil to avoid light exposure, in the presence or absence of 5-ALA for 6 h (24-26), and then, the cells were fixed and mounted. Cellular PpIX was analyzed using laser scanning microscopy (LSM 510 META, Carl Zeiss).

For the quantification of PpIX by fluorescence, we optimized a previously described method for quantifying 5-ALA-induced PpIX fluorescence (27). To determine the extracellular fluorescence intensity, the supernatant from incubated samples was removed for analysis. To determine the intracellular fluorescence intensity, cells were lysed and mixed with methanolic perchloric acid (5.6%, 8 °C). The fluorescence intensity was measured using a fluorescence microplate reader (Infinite M200, TECAN; Magellan^{TM} software) at an excitation wavelength of 400 ± 30 nm and an emission wavelength of 645 ± 40 nm. The relative fluorescence unit (RFU) values were standardized to total cellular protein and are shown as RFU/μg.

For the fluorescence-activated cell sorting (FACS) analysis, we used a FACS caliber instrument (BD Bioscience) with the laser set to a constant excitation intensity of 488 nm. The y-axis denotes the number of cells, and the x-axis indicates the fluorescence intensity (28).

In vitro experimental design for the measurement of intracellular concentrations of iron, heme, PpIX, and FECH.

Fig. 1 summarizes the in vitro experiments. First, the human glioblastoma cell line U-87 (ATCC) was cultured at 37 °C in a humidified CO_2 incubator with RPMI and 10% fetal bovine serum. The cells were incubated for 48 h with RPMI containing FAC(ferric ammonium citrate) (100 μM) for iron supplementation after the cell viability test, as analyzed by MTT assay (Sigma). Second, the cells were washed with PBS and incubated for 6 h in RPMI containing 5-ALA (500 μM) or not containing 5-ALA. Then, intracellular and extracellular PpIX was measured in the cells without exposure to FAC. Third, the medium was replaced with 5-ALA-free RPMI, and the cells were further incubated for 1, 24, or 48 h. The cells were harvested at 1, 24, or 48 h after incubation and were used to measure the intracellular concentrations of iron, heme, PpIX, and FECH.

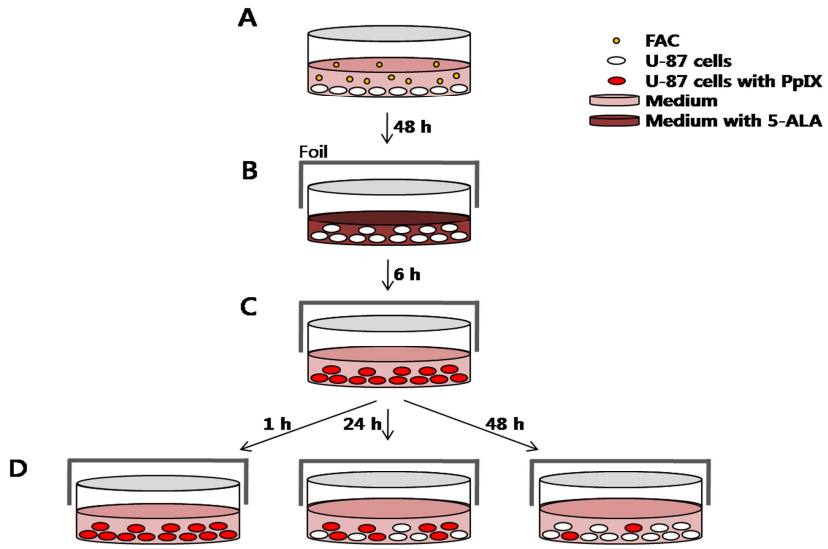

Fig. 1. In vitro experimental design for the measurement of intracellular concentrations of iron, heme, PpIX, and FECH. (*A*) Cells were incubated

with RPMI containing FAC for 48 h. (*B*) After washing with PBS, the medium was replaced with RPMI containing 5-ALA or the control, and the dish was wrapped in aluminum foil to avoid light exposure. (*C*) After incubation for 6 h, the medium was replaced with 5-ALA-free RPMI, and (*D*) the cells were further incubated for 1, 24, or 48 h. The cells were then used for the in vitro experiments.

Measurement of intracellular iron, heme, and PpIX at 1, 24 and, 48 h after exposure to 5-ALA.

Iron concentration was determined using a total iron reagent kit (Pointe Scientific). The production of heme in the cells was assayed using a commercially available kit (QuantiChrom ^{TM} Heme assay Kit, DIHM-250). The average concentrations of iron and heme were standardized to total cellular protein and are shown as μg/mg. The intracellular accumulation of PpIX was measured using fluorescence imaging, as described above.

Measurement of the intracellular concentration of FECH at 1, 24, and 48 h after exposure to 5-ALA.

The intracellular concentration of FECH was determined using a human FECH ELISA kit (Wuhan EIAab Science, E2083h). The intensity was measured in a microplate reader at 450 nm. The average concentrations were standardized to total cellular protein and are shown as ng/mg.

In Vivo Experiments.

These experiments were approved by the animal care committee at Seoul National University Hospital. A total of 10 mice with orthotopic brain tumors were used in this study. The mice received an oral administration of 5-ALA (0.1 mg/g body weight) (n = 6; 5-ALA group) or normal saline (n = 4; control group) 24 h before MRI. To produce mice with orthotopic brain tumors, 6-week-old male BALB/c nude mice were anesthetized by intraperitoneal injection with a mixture of zolazepam and xylazine and were placed in a stereotaxic device. U-87 glioma cells (1×10^6 cells/3 μl of serum free RPMI) were inoculated into the left caudate-putamen region. The cells were injected at a depth of 3 mm from the skull using a Hamilton syringe fitted with a 28-gauge needle, which was positioned with a syringe attachment fitted to the stereotaxic device. Three weeks after inoculation, we acquired images from anesthetized mice in a 7 T BioSpec MRI scanner (Bruker). MRI experiments were performed before and 24 h after the oral intake of 5-ALA or normal saline. Coronal slices were acquired at the site of the glioma cells using T_2-weighted spin-echo and T_2*-weighted gradient-echo sequences. For T_2-weighted imaging, the following acquisition parameters were used: TR/TE = 1500/35; matrix size = 256 × 256; field of view = 20 × 20 mm; slice thickness = 0.7 mm; and signal average factor = 8. For the estimation of T_2*, we used a gradient-echo pulse sequence with the following imaging parameters: TR/TE = 1500/2.76, 6.42, 10.08, 13.75, 17.41, 21.07, 24.73, 28.40 ms; flip angle (FA) = 30 °; field of view = 20 × 20 mm; matrix size = 256 × 256; slice thickness = 0.7 mm; pixel resolution = 0.08 × 0.08 mm; no intersection gap; and 1 signal average. In total, eight image slices were

collected per mouse. For the analysis of T_2* in the brain tumors, we used a previously described method (29). Regions of interest (ROIs) were defined in individual slices acquired at the shortest TE, and these data was used to generate T_2* maps of the ROIs using pixel-by-pixel analyses across the eight-point MRIs in MATLAB^{TM} (MathWorks Inc.), assuming single exponential decay (i.e., $SI = SI_0 \times e^{-TE/T2^*}$, where SI is the signal intensity and SI_0 is the proton density).

Histological analysis.

Mice undergoing MRI were sacrificed for histology. Before histological analysis, the brains were fixed in 10% buffered formalin. Paraffin-embedded brains were sectioned into 4 or 10 μm thick sections. Prussian blue staining of the 4 μm thick sections was used to visualize iron deposition.

Measurement of intratumoral iron concentrations using LA-ICP-MS.

We measured the intratumoral iron levels of the mice in the 5-ALA (n = 3) and control groups (n = 2) using LA-ICP-MS for brain sections. The analysis was performed using a New Wave Research UP-213 laser ablation instrument (Kennelec Technologies) fitted with a Large Format Cell. Argon was used as the carrier gas. The laser unit was hyphenated to an Agilent Technologies 7500cx ICP-MS instrument fitted with a 'cs' lens system, a platinum sampler, and skimmer cones. Prior to analysis, the system was tuned for sensitivity using a NIST 612 Trace element in glass and in-house-produced tissue standards. Oxide formation was controlled by limiting the amount of ^{232}Th16O+/^{232}Th+ to < 0.3% for the ablation of NIST 612.

Data were acquired by ablating adjacent lines down each specimen (10 μm thick) with a beam diameter of 100 μm and a scan speed of 300 μm s^{-1}. Mass spectrometer integration times were chosen in order to maintain the true image dimensions (30) when processed, such that a single pixel represented 100 μm^2. Variation in laser power output and instrument drift was compensated for through normalization to the ^{13}C signal (31).

Quantitative data were produced through representative ablation of tissue standards, using a previously described method (32, 33). Briefly, chicken breast tissue was purchased from a local market and stripped of all fatty and connective tissue. Five-gram aliquots of dissected tissue were partially homogenized using an OmniTech TH tissue homogenizer (Kelly Scientific) fitted with a polycarbonate probe. Then, 10 to 100 μL aliquots of standard metal solutions were prepared from high-purity iron-nitrate salts (Sigma-Aldrich) and added to each standard preparation, which were then further homogenized. Next, six approximately 250 mg aliquots of each standard were digested in HNO3:H2O2 (3:1 ratio) in a Milestone MLS 1200 microwave digester (John Morris Scientific), and each standard was analyzed by solution nebulization ICP-MS to accurately determine the trace metal concentration and homogeneity.

Data were reduced into multispectral images using the Interactive Data Imaging Spectral Data Analysis Software (ISIDAS) developed by the University of Technology, Sydney Computational Research Support Unit. ISIDAS is a specialized data reduction package written in the Python programming language. Images were exported from ISIDAS in a Visualization Toolkit (.vtk) format into Enthought MayaVi2 for color rendering. Quantitative data were extracted by freehand outlining of the ROIs using ISIDAS.

Results

In Vitro Experiments.

Monitoring PpIX Synthesis by 5-ALA in U-87 Glioblastoma Cells.

To measure the synthesis of PpIX by 5-ALA, U-87 cells were incubated with 5-ALA for 6 h without exposure to FAC. Confocal laser scanning microscopy revealed defined red fluorescence in the cytoplasm of cells treated with 5-ALA in comparison to untreated cells (Fig. 2). Following treatment of cells with 5-ALA, the intracellular PpIX concentration was significantly increased as compared to that in untreated control cells (203.3 ± 3.6 RFU/μg vs. 17.2 ± 1.2, $P < 0.001$). Moreover, the extracellular concentration of PpIX in the medium from cells treated with 5-ALA was also higher than that detected in the medium from untreated control cells (18.5 ± 1.1 vs. 11.4 ± 0.4, $P < 0.001$). However, the intracellular concentration of PpIX was much higher than the extracellular concentration of PpIX, which suggests that PpIX has low diffusion kinetics from the intracellular to the extracellular space following treatment with 5-ALA (Fig. 3). FACS analysis revealed increased fluorescence in over 80% of the cells treated with 5-ALA, which was indicative of PpIX synthesis, whereas less than 1% of the untreated control cells demonstrated fluorescence (81.29 ± 0.54% vs. 0.88 ± 0.05%, $P = 0.0286$) (Fig. 4).

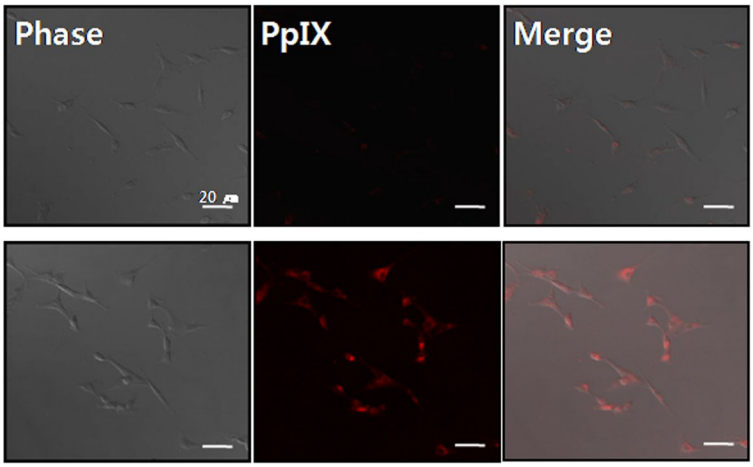

Fig. 2. Confocal laser scanning microscopy images of U-87 cells left untreated (upper) or treated with 500 μM 5-ALA (lower) for 6 h. PpIX, which could be visualized as red fluorescence, was located mainly in the cytoplasm

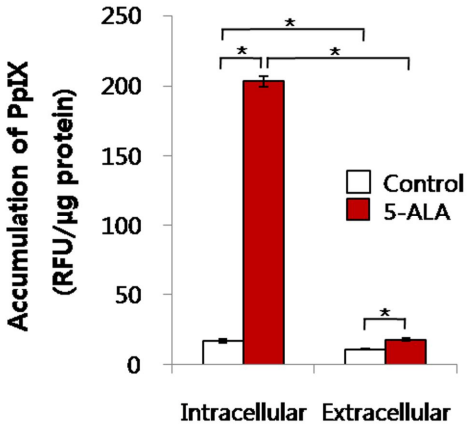

Fig. 3. Measurement of intracellular PpIX accumulation in cells treated with 5-ALA for 6 h. The intracellular PpIX concentration of cells treated with 5-ALA was significantly higher than that of untreated control cells ($P < 0.001$). Moreover, the intracellular concentration of PpIX was much higher than the extracellular concentration of PpIX.

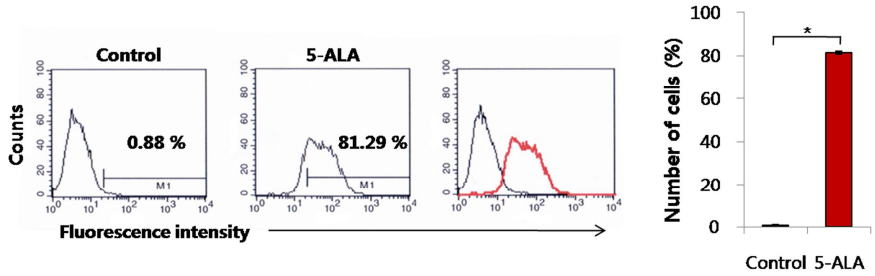

Fig. 4. Fluorescence intensity of intracellular PpIX accumulation in cells treated with 5-ALA. Over 80% of the cells treated with 5-ALA showed an increase in fluorescence, while less than 1% of the untreated cells demonstrated fluorescence ($P = 0.0286$).

Measurement of Intracellular Iron, Heme, and PpIX at 1, 24, and 48 h after Treatment with 5-ALA.

In cells treated with or without 5-ALA, the concentration of intracellular iron increased significantly ($P < 0.05$) over time (1, 24, and 48 h) (Fig. 5*A*). However, at 24 h, the concentration of intracellular iron was higher in cells exposed to 5-ALA than in untreated cells (1.95 ± 0.07 vs. 1.67 ± 0.07 μg/mg, $P < 0.05$) (Fig. 5*A*).

The concentration of intracellular heme also increased significantly ($P < 0.05$) over time (1, 24, and 48 h) in cells treated with or without 5-ALA (Fig. 5*B*). At 24 h, a significant difference was also observed between the cells treated with and without 5-ALA (1.19 ± 0.07 vs. 0.86 ± 0.11 μg/mg, $P < 0.001$) (Fig. 5*B*). Furthermore, the intracellular concentration of PpIX increased dramatically within 1 h after exposure to 5-ALA but decreased by 24 and 48 h after treatment (Fig. 5*C*).

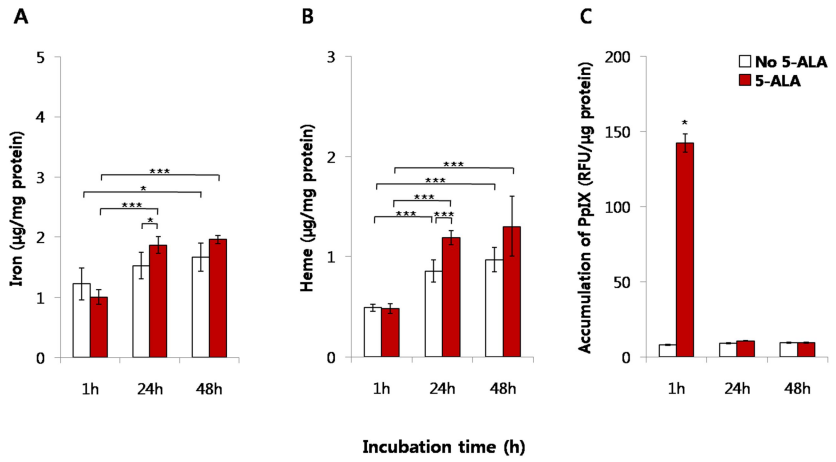

Fig. 5. The measurement of intracellular iron, heme, and PpIX after incubation with 5-ALA for 1, 24, and 48 h. (*A*) The intracellular iron content of cells exposed to 5-ALA was higher than that of control cells at 24 h ($P < 0.05$). (*B*) Levels of intracellular heme also increased significantly ($P < 0.05$) over time in both cells treated with 5-ALA and the control. At 24 h, the heme values were significantly different between cells treated with 5-ALA and those left untreated ($P < 0.001$). (*C*) The intracellular PpIX concentration was increased at 1 h after exposure to 5-ALA but had decreased by 24 and 48 h. *$P < 0.05$; **$P < 0.01$; ***$P < 0.001$.

Measurement of FECH at 1, 24, and 48 h after Treatment with 5-ALA.

Following treatment with 5-ALA, the highest intracellular concentration (0.315 ng/mg protein) of FECH was observed at 24 h ($P < 0.01$). At both 24 and 48 h, the intracellular concentration of FECH was higher in cells treated with 5-ALA than in those not treated with 5-ALA ($P < 0.001$) (Fig. 6).

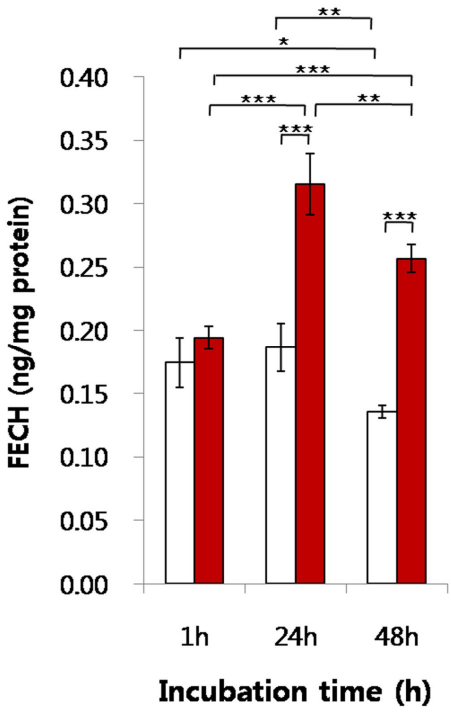

Fig. 6. The measurement of FECH following incubation with 5-ALA for 1, 24, and 48 h. Treatment with 5-ALA resulted in the greatest intracellular concentration of FECH at 24 h posttreatment ($P < 0.01$), whereas the concentration of FECH had decreased significantly at 48 h in untreated cells ($P < 0.05$). However, at 24 and 48 h, the intracellular concentration of FECH was higher in cells treated with 5-ALA as compared those left untreated ($P < 0.001$). *$P < 0.05$; **$P < 0.01$; ***$P < 0.001$.

In Vivo Experiments.

In Vivo MRI of U-87 Glioblastoma Tumors after Treatment with 5-ALA.

T_2* mapping showed that the mean T_2* value of U-87 glioblastoma tumors treated with 5-ALA was lower than that of control tumors, which received normal saline (14.9 ± 1.2 vs. 21.4 ± 2.6 ms, $P < 0.0001$) (Fig. 7).

There was no significant difference between the mean T_2* values of brain tumors before and after the administration of saline (22.4 ± 2.5 vs. 21.4 ± 2.6 ms, P = 0.6857; Fig. 7*A*). However, T_2* histograms showed that the number of pixels with low T_2* was higher in brain tumors 24 h after receiving 5-ALA as compared to the number measured prior to treatment. Finally, the mean T_2* value of brain tumors significantly decreased following treatment with 5-ALA (20.6 ± 1.1 vs. 14.9 ± 1.2 ms, P < 0.0001; Fig. 7*B*).

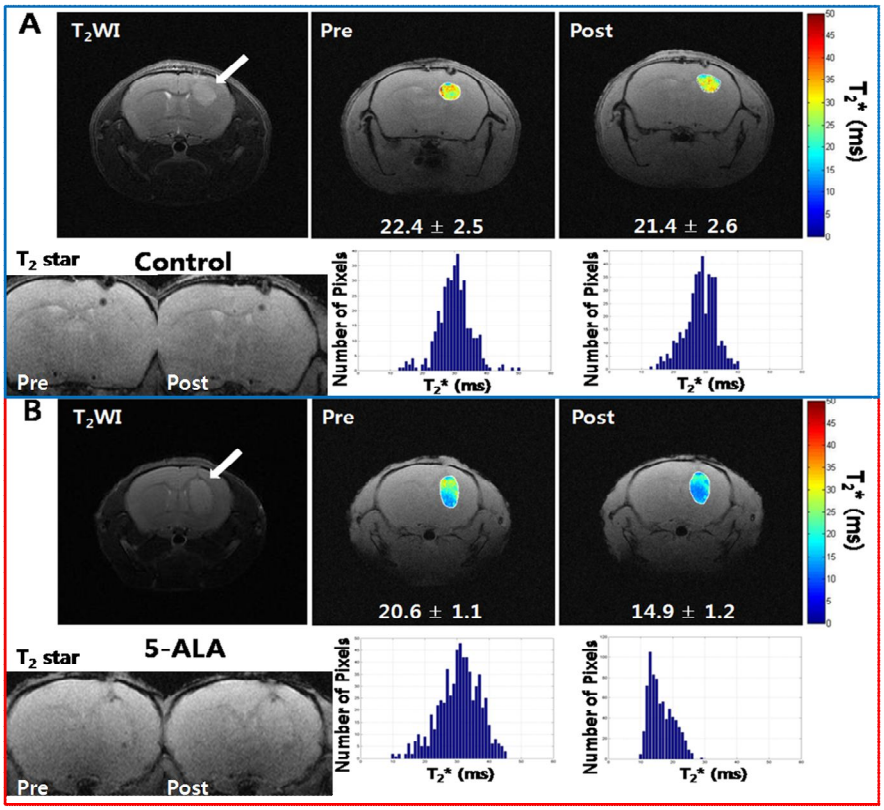

Fig. 7. MRI detection of heme synthesized as a result of PpIX generated by 5-ALA treatment in U-87 glioblastomas. (*A*, *B*) The number of pixels (blue bars) was used to calculate the mean T_2* value, and these values were used for the detection of heme-induced changes in T_2*. The mean

T_2* value of U-87 glioblastomas treated with 5-ALA was lower than that of control tumors, which received normal saline ($P < 0.0001$). (*A*) T_2* maps showed no significant difference between the mean T_2* values of brain tumors before and after receiving saline ($P = 0.6857$). (*B*) However, the mean T_2* value of brain tumors significantly decreased following treatment with 5-ALA ($P < 0.0001$). The arrow indicates the U-87 glioblastoma in the mouse brain. Note that it was impossible to perceive signal change between pre and post T_2* image(left lower), compared with difference of T_2* value.

Histological Results.

Prussian blue staining revealed multifocal iron deposits (arrow) at the border (dotted line) between the tumor and the brain in mice treated with 5-ALA. However, no staining of iron deposits was observed in control mice treated with saline (Fig. 8*A*).

Intratumoral Iron Level Measured by LA-ICP-MS.

A significant difference in the mean concentration of iron was observed between the control animals and the 5-ALA-treated animals (41.4 ± 0.9 μg/g vs. 60.1 ± 2.2 μg/g, $P < 0.0001$; Fig. 8*B*).

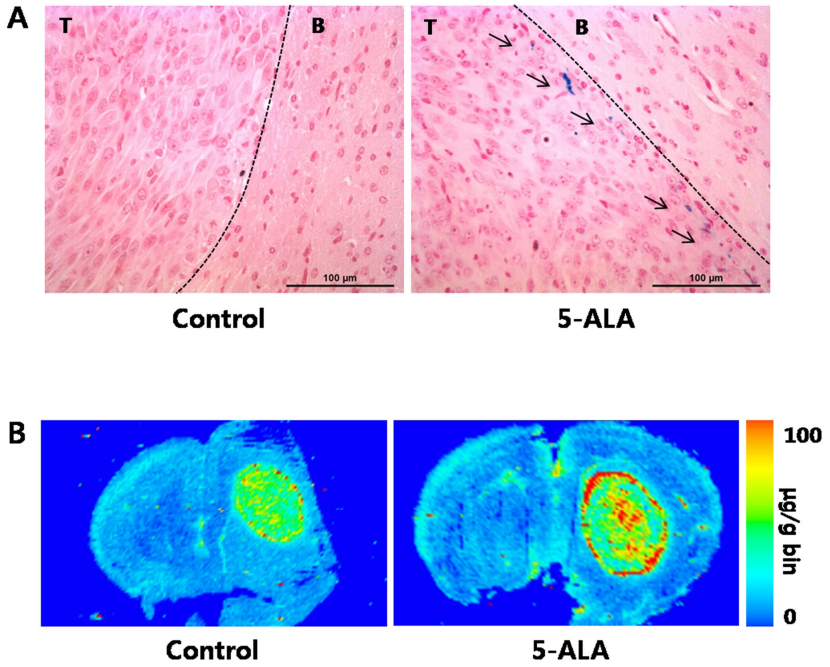

Fig. 8. Determination of heme iron in brain tumors by histological analysis. (*A*) Multifocal iron deposits (arrow) at the border (dotted line) between the tumor and the brain in mice treated with 5-ALA were stained by Prussian blue. No staining was observed in the control mice treated with saline. (*B*) Intratumoral iron levels showed a significant difference in the mean concentration of iron between the control animals and the 5-ALA-treated animals, as measured by LA-ICP-MS (41.4 ± 0.9 μg/g vs. 60.1 ± 2.2 μg/g, $P < 0.0001$). T, tumor; B, brain.

Discussion

In the present study, we observed a significant accumulation of iron in response to 5-ALA induced heme synthesis in malignant glioblastomas as compared to control glioblastoma cells and tumors. One previous study showed that decreased FECH expression in malignant gliomas was correlated with intracellular PpIX accumulation (34). However, no data have been reported concerning measurements of iron metabolism within glioblastoma cells following the administration of 5-ALA, even though the use of 5-ALA-induced fluorescence has been well established for glioblastoma resection. In this study, U-87 glioblastoma cells demonstrated the highest concentration of PpIX at 1 h after 6 h of exposure to 5-ALA, and the concentration of PpIX subsequently decreased by 24 and 48 h after exposure. The intracellular concentration of the both heme and iron were increased at both 24 and 48 h after 5-ALA exposure. In addition, 5-ALA promoted the in vitro expression of FECH in U-87 glioblastoma cells, and this expression level was higher at 24 and 48 h after 5-ALA exposure as compared to 1 h after exposure. FECH is likely responsible for iron accumulation in U-87 glioblastoma cells. In vivo MRI revealed a lower T_2* value in U-87 glioblastomas from mice treated with 5-ALA as compared to control mice, and in vitro LA-ICP-MS also revealed that the iron concentrations were increased in U-87 glioblastomas from mice following exposure to 5-ALA. Thus, using both in vitro and in vivo models, this study is the first to demonstrate that the intracellular iron concentration in glioblastomas increases following exposure to 5-ALA.

5-ALA is a precursor in the hemoglobin synthesis pathway, and

exogenous, oral administration of this molecule several hours before surgery leads to the preferential accumulation of PpIX within tumor cells (35). Preclinical and clinical studies suggest that the accumulation of PpIX in glioblastoma cells may be caused by various factors (36). As the normal blood–brain barrier (BBB) is impermeable to 5-ALA, the compromised BBB in glioblastoma tissue is required for 5-ALA to cross and make contact with glioblastoma cells. 5-ALA enters tumor cells through transporters, such as peptide transporter 2, which is the primary transporter responsible for 5-ALA uptake in astrocytes (37, 38). Furthermore, the study by Teng *et al*. demonstrated that FECH mRNA expression was significantly downregulated in glioblastomas as compared to normal brain tissues (34). Also in this study, SNB19 cells, which express lower levels of FECH than G112 cells, accumulated more PpIX than G112 cells following exposure to 5-ALA, and there was a correlation between FECH expression and PpIX accumulation. In practice, 5-ALA is given to patients orally at 2.5 to 3.5 h before the administration of anesthesia. Under blue-violet light, the fluorophore, PpIX, emits light in the red region of the visible spectrum, enabling the identification of tumor tissue that might otherwise be difficult to distinguish from normal brain tissue (35). The time point of administration used in this study was derived from initial in vivo experiments using the C6 glioma model in rats. In these experiments, maximal PpIX fluorescence was observed approximately 6 h after administration, whereas the fluorescence was decreased after 3 and 9 h (13). We also observed a similar change in PpIX fluorescence in U-87 cells after exposure to 5-ALA. In addition, these U-87 cells showed an increase in the concentration of both intracellular iron and heme 24 h after exposure to 5-ALA. Thus, we believe that 5-ALA

exposure can increase FECH expression to stimulate the metabolism of PpIX to heme within glioblastoma cells, a process that takes approximately 6 to 24 h.

In routine neurosurgical practice, MRI contrast enhancement is used to visualize the most malignant areas of a tumor. However, in diffusely infiltrating WHO grade II and III gliomas, such contrast uptake is frequently not observed; the absence of significant contrast enhancement was reported in up to 55% of WHO grade III gliomas and up to 56% of low-grade gliomas using contrast media with MRI (1). Thus, 5-ALA-induced fluorescence may be effective for guiding the surgical resection of high-grade glioma in these patients. Furthermore, some high-grade gliomas can be positive for 5-ALA-fluorescence without demonstrating contrast enhancement on MRI. Because 5-ALA is a small, but polar, amino acid, its uptake into the brain may depend on slight perturbations in the integrity of the BBB, although not as severe as those necessary for gadolinium to enter the brain (39). In the present study, in vivo MRI revealed a significant decrease in the T_2* values of glioblastomas 24 h after the oral administration of 5-ALA as compared to both baseline MRI and MRI values obtained from mice in the control group. Within glioblastoma cells, heme is generated via the incorporation of Fe^{2+} into the metabolite of 5-ALA, PpIX, by FECH (21). Thus, we believe that Fe^{2+} incorporation into heme is a major contributor to the T_2* contrast of in vivo MRI. Our results suggest that 5-ALA can be used for the detection of malignant foci within gliomas using MRI, especially for postoperative evaluation and follow-up MRI. It has also been reported that tumor resection guided by 5-ALA-induced fluorescence can result in incomplete resection for patients with malignant gliomas with satellite lesions (40).

In the present study, we utilized LA-ICP-MS with an in vivo model of glioblastoma to examine iron concentrations in brain sections after MRI. LA-ICP-MS can be used for the in situ analysis of trace metals in biological tissue, and ICP-MS is an element analyzer that is designed to measure trace levels of elements, unlike other forms of "organic" MS, which are used to identify and quantify molecular compounds. Furthermore, laser ablation is a sample introduction system for ICP-MS that enables the determination of the elemental composition of solid materials, including tissues (32). The iron concentration of glioblastomas exposed to 5-ALA was higher than that of glioblastomas in the control group, which correlated with the MRI results. The LA-ICP-MS results further support the hypothesis that the decreased T_2* value of glioblastomas exposed to 5-ALA was due to the increased iron concentration within the tumors.

In conclusion, this study is the first to demonstrate that 5-ALA administration increases the intracellular iron concentration of glioblastomas by promoting the synthesis of heme, which is the metabolite of 5-ALA. As intracellular iron can be detected by MRI, we believe that 5-ALA-enhanced MRI will aid in the identification of high-grade foci in gliomas.

References

1. Widhalm G, Wolfsberger S, Minchev G, Woehrer A, Krssak M, Czech T, et al. 5-Aminolevulinic acid is a promising marker for detection of anaplastic foci in diffusely infiltrating gliomas with nonsignificant contrast enhancement. *Cancer. 2010;116:1545-52*.
2. Jansen EP, Dewit LG, van Herk M, Bartelink H. Target volumes in radiotherapy for high-grade malignant glioma of the brain. Radiotherapy and oncology : *journal of the European Society for Therapeutic Radiology and Oncology. 2000;56:151-6.*
3. Watanabe M, Tanaka R, Takeda N. Magnetic resonance imaging and histopathology of cerebral gliomas. *Neuroradiology. 1992;34:463-9.*
4. Kang Y, Choi SH, Kim YJ, Kim KG, Sohn CH, Kim JH, et al. Gliomas: Histogram analysis of apparent diffusion coefficient maps with standard- or high-b-value diffusion-weighted MR imaging–correlation with tumor grade. *Radiology. 2011;261:882-90.*
5. Arvinda HR, Kesavadas C, Sarma PS, Thomas B, Radhakrishnan VV, Gupta AK, et al. Glioma grading: sensitivity, specificity, positive and negative predictive values of diffusion and perfusion imaging. *J Neurooncol. 2009;94:87-96.*
6. Kim JH, Chang KH, Na DG, Song IC, Kwon BJ, Han MH, et al. 3T 1H-MR spectroscopy in grading of cerebral gliomas: comparison of short and intermediate echo time sequences. *AJNR Am J Neuroradiol. 2006;27:1412-8.*
7. Floeth FW, Pauleit D, Wittsack HJ, Langen KJ, Reifenberger G, Hamacher K, et al. Multimodal metabolic imaging of cerebral

gliomas: positron emission tomography with [18F]fluoroethyl-L-tyrosine and magnetic resonance spectroscopy. *Journal of neurosurgery. 2005;102:318-27.*

8. Stadlbauer A, Prante O, Nimsky C, Salomonowitz E, Buchfelder M, Kuwert T, et al. Metabolic imaging of cerebral gliomas: spatial correlation of changes in O-(2-18F19 fluoroethyl)-L-tyrosine PET and proton magnetic resonance spectroscopic imaging. *J Nucl Med. 2008;49:721-9.*

9. Roessler K, Gatterbauer B, Becherer A, Paul M, Kletter K, Prayer D, et al. Surgical target selection in cerebral glioma surgery: linking methionine (MET) PET image fusion and neuronavigation. *Minimally invasive neurosurgery : MIN. 2007;50:273-80.*

10. Singhal T, Narayanan TK, Jain V, Mukherjee J, Mantil J. 11C-L-methionine positron emission tomography in the clinical management of cerebral gliomas. Molecular imaging and biology : *MIB : the official publication of the Academy of Molecular Imaging. 2008;10:1-18.*

11. Goldman S, Levivier M, Pirotte B, Brucher JM, Wikler D, Damhaut P, et al. Regional methionine and glucose uptake in high-grade gliomas: a comparative study on PET-guided stereotactic biopsy. *J Nucl Med. 1997;38:1459-62.*

12. Sadeghi N, Salmon I, Decaestecker C, Levivier M, Metens T, Wikler D, et al. Stereotactic comparison among cerebral blood volume, methionine uptake, and histopathology in brain glioma. *AJNR Am J Neuroradiol. 2007;28:455-61.*

13. Stummer W, Stocker S, Novotny A, Heimann A, Sauer O, Kempski O, et al. In vitro and in vivo porphyrin accumulation by

C6 glioma cells after exposure to 5-aminolevulinic acid. *Journal of photochemistry and photobiology B, Biology. 1998;45:160-9.*

14. Stummer W, Pichlmeier U, Meinel T, Wiestler OD, Zanella F, Reulen HJ. Fluorescence-guided surgery with 5-aminolevulinic acid for resection of malignant glioma: a randomised controlled multicentre phase III trial. *Lancet Oncol. 2006;7:392-401.*
15. Hefti M, von Campe G, Moschopulos M, Siegner A, Looser H, Landolt H. 5-aminolevulinic acid induced protoporphyrin IX fluorescence in high-grade glioma surgery: aone-year experience at a single institutuion. *Swiss medical weekly. 2008;138:180-5.*
16. Ishihara R, Katayama Y, Watanabe T, Yoshino A, Fukushima T, Sakatani K. Quantitative spectroscopic analysis of 5-aminolevulinic acid-induced protoporphyrin IX fluorescence intensity in diffusely infiltrating astrocytomas. *Neurol Med Chir (Tokyo). 2007;47:53-7; discussion 7.*
17. Utsuki S, Oka H, Sato S, Suzuki S, Shimizu S, Tanaka S, et al. Possibility of using laser spectroscopy for the intraoperative detection of nonfluorescing brain tumors and the boundaries of brain tumor infiltrates. Technical note. *Journal of neurosurgery. 2006;104:618-20.*
18. Berlin NI, Neuberger A, Scott JJ. The metabolism of delta - aminolaevulic acid. 1. Normal pathways, studied with the aid of 15N. *The Biochemical journal. 1956;64:80-90.*
19. Berlin NI, Neuberger A, Scott JJ. The metabolism of delta - aminolaevulic acid. 2. Normal pathways, studied with the aid of 14C. *The Biochemical journal. 1956;64:90-100.*
20. Ryter SW, Tyrrell RM. The heme synthesis and degradation

pathways: role in oxidant sensitivity. Heme oxygenase has both pro- and antioxidant properties. *Free radical biology & medicine. 2000;28:289-309.*

21. Chen YH, Yet SF, Perrella MA. Role of heme oxygenase-1 in the regulation of blood pressure and cardiac function. *Exp Biol Med (Maywood). 2003;228:447-53.*

22. Schenck JF. Magnetic resonance imaging of brain iron. *J Neurol Sci. 2003;207:99-102.*

23. Schenck JF. Imaging of brain iron by magnetic resonance: T2 relaxation at different field strengths. *J Neurol Sci. 1995;134 Suppl:10-8.*

24. Millon SR, Ostrander JH, Yazdanfar S, Brown JQ, Bender JE, Rajeha A, et al. Preferential accumulation of 5-aminolevulinic acid-induced protoporphyrin IX in breast cancer: a comprehensive study on six breast cell lines with varying phenotypes. *Journal of biomedical optics. 2010;15:018002.*

25. Gibbs SL, Chen B, O'Hara JA, Hoopes PJ, Hasan T, Pogue BW. Protoporphyrin IX level correlates with number of mitochondria, but increase in production correlates with tumor cell size. *Photochemistry and photobiology. 2006;82:1334-41.*

26. Wu SM, Ren QG, Zhou MO, Wei Y, Chen JY. Photodynamic effects of 5-aminolevulinic acid and its hexylester on several cell lines. Sheng wu hua xue yu sheng wu wu li xue bao *Acta biochimica et biophysica Sinica. 2003;35:655-60.*

27. Hefti M, Holenstein F, Albert I, Looser H, Luginbuehl V. Susceptibility to 5-aminolevulinic acid based photodynamic therapy in WHO I meningioma cells corresponds to ferrochelatase

activity. *Photochemistry and photobiology. 2011;87:235-41.*

28. Oriel S, Nitzan Y. Photoinactivation of Candida albicans by its own endogenous porphyrins. *Current microbiology. 2010;60:117-23.*

29. Choi SH, Cho HR, Kim HS, Kim YH, Kang KW, Kim H, et al. Imaging and quantification of metastatic melanoma cells in lymph nodes with a ferritin MR reporter in living mice. *NMR Biomed. 2011.*

30. Lear J, Hare D, Adlard P, Finkelstein D, Doble P. Improving acquisition times of elemental bio-imaging for quadrupole-based LA-ICP-MS. *J Anal Atom Spectrom. 2012;27:159-64.*

31. Austin C, Fryer F, Lear J, Bishop D, Hare D, Rawling T, et al. Factors affecting internal standard selection for quantitative elemental bio-imaging of soft tissues by LA-ICPMS. *J Anal Atom Spectrom. 2011;26:1494-501.*

32. Hare D, Reedy B, Grimm R, Wilkins S, Volitakis I, George JL, et al. Quantitative elemental bio-imaging of Mn, Fe, Cu and Zn in 6-hydroxydopamine induced Parkinsonism mouse models. *Metallomics. 2009;1:53-8.*

33. Hare DJ, George JL, Grimm R, Wilkins S, Adlard PA, Cherny RA, et al. Threedimensional elemental bio-imaging of Fe, Zn, Cu, Mn and P in a 6-hydroxydopamine lesioned mouse brain. *Metallomics. 2010;2:745-53.*

34. Teng L, Nakada M, Zhao SG, Endo Y, Furuyama N, Nambu E, et al. Silencing of ferrochelatase enhances 5-aminolevulinic acid-based fluorescence and photodynamic therapy efficacy. *Br J Cancer. 2011;104:798-807.*

35. Roberts DW, Valdes PA, Harris BT, Hartov A, Fan X, Ji S, et al. Glioblastoma multiforme treatment with clinical trials for surgical resection (aminolevulinic Acid). *Neurosurgery clinics of North America. 2012;23:371-7.*

36. Norum OJ, Selbo PK, Weyergang A, Giercksky KE, Berg K. Photochemical internalization (PCI) in cancer therapy: from bench towards bedside medicine. *Journal of photochemistry and photobiology B, Biology. 2009;96:83-92.*

37. Rodriguez L, Batlle A, Di Venosa G, MacRobert AJ, Battah S, Daniel H, et al. Study of the mechanisms of uptake of 5-aminolevulinic acid derivatives by PEPT1 and PEPT2 transporters as a tool to improve photodynamic therapy of tumours. *The international journal of biochemistry & cell biology. 2006;38:1530-9.*

38. Xiang J, Hu Y, Smith DE, Keep RF. PEPT2-mediated transport of 5-aminolevulinic acid and carnosine in astrocytes. *Brain Res. 2006;1122:18-23.*

39. Ewelt C, Floeth FW, Felsberg J, Steiger HJ, Sabel M, Langen KJ, et al. Finding the anaplastic focus in diffuse gliomas: the value of Gd-DTPA enhanced MRI, FET-PET, and intraoperative, ALA-derived tissue fluorescence. *Clinical neurology and neurosurgery. 2011;113:541-7.*

40. Tsugu A, Ishizaka H, Mizokami Y, Osada T, Baba T, Yoshiyama M, et al. Impact of the combination of 5-aminolevulinic acid-induced fluorescence with intraoperative magnetic resonance imaging-guided surgery for glioma. *World neurosurgery. 2011;76:120-7.*

국문초록

서론: 이 실험은 자기공명영상(MRI)를 이용하여 뇌종양의 악성 부분을 영상화하는 새로운 기술 개발을 목표로 하였다. 5-아미노레불린산(5-ALA)을 주입하면 프로토포르피린 IX(protoporphyrin IX, PpIX)이라는 형광 물질이 악성 신경교종에 축적되게 되며, 이를 이용해서 광범위적으로 침습적인 신경교종 수술에서 악성 부분을 찾을 수 있다. 프로토포르피린 IX는 미토콘드리아의 페로케라타아제(ferrochelatase, FECH)에 의해 철(ferrous iron)과 결합하여 헴(heme)으로 합성된다. 이와 같은 대사 과정이 있음을 바탕으로 5-ALA의 주입 후 헴(heme)의 합성이 악성 신경교종에서 증가 함을 증명하고, 헴의 초상자성(superparamagnetic)을 이용하여, 헴이 축적된 악성 종양 부분을 자기공명영상으로 영상화 하기 위해 생체외 실험과 생쥐 뇌 악성종양 모델을 이용한 생체내 실험을 계획하였다.

방법: 생체외 실험에서는 사람 악성 신경교종 세포주 U-87에 5-아미노레불린산을 처리한 군과 처리하지 않은 군으로 실험 군을 나누었으며, 각 세포군에서 1, 24, 48시간 후의 세포내 철, 헴, 프로토포프피린 IX, 페로케라타아제의 양을 측정하였다.

생쥐 뇌 악성 종양 모델 총 10마리를 이용하여 생체내 실험을 수행하였다. 이중 6마리는 자기공명영상 촬영 24시간 전에 5-아미노레불린산을 경구로 투여받았고, 4마리는 식염수를 경구로

투여 받았다. 자기공명영상은 종양이 있는 부분을 중심으로 관상면으로 T2와 T2* 강조영상 촬영하였고, 이를 MATLAB™ (MathWorks Inc.)프로그램을 이용한 ROI 픽셀 분석으로 T2* 지도 영상을 생성하여 분석하였다.

마지막으로 종양 조직을 적출하여 병리적 염색과 세포 내의 철을 정량화하는 방법으로 종양조직 내 철의 축적을 확인 및 비교하였다.

결과: 생체외 실험 5-아미노레블린산을 노출되었던 세포군에서 노출 후 24시간 후 세포내 철과 헴의 양이 노출되지 않았던 세포군에 비하여 통계적으로 의미있게 높았다 (1.95 ± 0.07 vs. 1.67 ± 0.07 μg/mg, $P < 0.05$ and 1.19 ± 0.07 vs. 0.86 ± 0.11 μg/mg, $P < 0.001$). 세포내 프로토포르피린 IX의 양은 5-아미노레불린산에 노출 후 1시간에 가장 높았고, 이후에는 급격하게 감소하는 양상을 보였다. 세포내 페로케라타아제의 양은 5-아미노레불린산에 노출 후 24시간에 가장 높았으며, 24, 48시간 모두에서 5-아미노레불린산을 노출되지 않았던 세포군보다 높았다.

5-아미노레불린산을 투여 받았던 생쥐 뇌 악성 종양 모델군에서 T2* 평균 값이 생리 식염수를 투여 받았던 대조군 보다 통계적으로 낮게 측정되었다(14.9 ± 1.2 vs. 21.4 ± 2.6 ms, $P < 0.0001$). 또한 5-아미노레불린산을 투여 받기 전 T2* 값에 비하여 통계적으로 유의하게 투여 후 T2* 값이 감소하였다. 마지막으로 종양 적출 후 측정한 종양 내 철 농도는 유의하게 대조군 보다 높았다.

결론: 5-아미노레불린산의 투여 후, 악성 신경교종에 헴의 축적이 유의하게 증가함을 확인할 수 있었으며, 이에 의하여 자기공명영상 T2* 신호의 감소를 확인할 수 있었다. 따라서 앞으로 5-아미노레불린산 이용한 자기공명영상이 광범위적으로 침습적인 신경교종에서 악성 부분을 찾아내는데 유용한 기술이 될 가능성이 있으며, 인간 대상 연구에서도 여러 분야에 이용 될 수 있을 것이다.

주요어: 5-아미노레불린산
악성 신경교종
프로토포르피린 IX
헴
자기공명영상

학 번: 2011-21824